Journal of Building Engineering 57 (2022) 104927

Contents lists available at ScienceDirect

Journal of Building Engineering

journal homepage: www.elsevier.com/locate/jobe

Demand response strategy applied to planning the operation of an air conditioning system. Application to a medical center

S.N. Bragagnolo [a,*], R.M. Schierloh [b], J.R. Vega [c,d], J.C. Vaschetti [a]

[a] Universidad Tecnológica Nacional, Facultad Regional Córdoba, CIDTIEE, Argentina
[b] Universidad Tecnológica Nacional, Facultad Regional Paraná, GiEPi, Argentina
[c] Universidad Tecnológica Nacional, Facultad Regional Santa Fe, CIESE, Argentina
[d] CONICET-UNL, INTEC, Santa Fe, Argentina

ARTICLE INFO

Keywords:
Demand response
Demand side management
HVAC management
Power optimization
Genetic algorithm
Thermal model

ABSTRACT

Large air conditioning systems, such as those used in shopping and health centers, typically demand high amounts of energy. Several air conditioning technologies and energy management strategies seek to minimize consumption to reduce billing expenses and improve system efficiency. This work proposes a demand response framework to plan the daily operation of an air conditioning system with the aim of minimizing the energy cost and guaranteeing thermal comfort. The framework includes an electrical-analogous thermal model, the formulation of the energy optimization problem with thermal and electrical constraints. The ISO 7730 standard is used to evaluate thermal comfort. The approach is applied to the air conditioning system of a radiotherapy and medical imaging center in Argentina. The optimization problem is solved through a genetic algorithm. To evaluate the strategy, two scenarios with different power demands are proposed: Case 1 (with demands lower than 300 kW) and Case 2 (with a peak demand greater than 300 kW). The results are compared with those obtained from an on-off strategy control with hysteresis. Penalties for large demands are avoided in Case 2, and therefore an economic saving of ≅ 16.8% is achieved. The thermal comfort is improved in both cases, with thermal cost reduction of 40.6% and 29.2% for Cases 1 and 2, respectively.

1. Introduction

The global increase in energy consumption, as well as its generation mainly from non-renewable energy sources, poses undoubted challenges. While distributed generation based on renewable sources allow the reduction of gas emissions, demand side management (DSM) strategies aim to manage the reduction of energy consumption. DSM involves load control of an electrical system to improve supply and sustainability by reducing consumption and temporarily shifting loads [1]. Moreover, DSM includes demand response (DR) programs, based on tariff schemes that encourage users to change their consumption habits and to improve energy efficiency [2].

DSM strategies require knowledge about the consumption pattern of each user, disaggregating the loads based on their magnitude and nature, to determine the feasibility of modifying the consumptions. In this sense, HVAC (heating, ventilation, and air conditioning) systems are responsible for a large part of the energy consumed in households, industries, and companies [3]. The energy consumed by fans and air conditioning (AC) represents 20% of the electrical demand of buildings and 10% of the global energy demand [4]. Some strategies can be implemented to reduce the consumption of HVAC systems to reach a more efficient operation. It is important to

* Corresponding author.
E-mail address: sbragagnolo@frc.utn.edu.ar (S.N. Bragagnolo).

https://doi.org/10.1016/j.jobe.2022.104927
Received 25 March 2022; Received in revised form 29 June 2022; Accepted 5 July 2022
Available online 8 July 2022

calculate the cooling and/or heating loads for the correct sizing, selection, and control of HVAC equipment. Any improvement in the calculation methods and in the real time prediction of the loads would imply a significant reduction in the energy consumed [5].

Several studies on DSM have considered HVAC systems as a controllable load and somehow included comfort in the objective function of the optimization problem. Heuristic optimization methods are often used due to the complexity of the problem. Most researchers focused on residential houses. A Mixed Integer Linear Programming (MILP) was used to improve cost while keeping the temperature within a given range [6]. The user can set the desired temperature, and the thermal discomfort level is quantified by the deviation of the indoor temperature with respect to the set-point value. This thermal discomfort was weighted in the objective function according to the user preferences. The authors of [7] proposed a two-stage stochastic programming to handle DR uncertainties in a commercial campus. The optimization objective function included the reduction of costs and the maximization of comfort. In a similar work [8], an evolutionary algorithm was used to minimize the cost and the difference between the desired and the measured temperatures. In Ref. [9], a distributed algorithm integrated the optimal price with the demand schedule to optimize the cost while temperature was considered as a linear constraint. A single-objective MILP algorithm was used to optimize the cost when the room temperature was forced to follow a linear function [10].

The MATLAB's YALMIP toolbox was used to solve a multi-objective optimization that considered cost and comfort, while the temperature was a linear function of the thermal resistance [11]. A three-layer control system was proposed to optimize the available energy and thermal comfort [12]. To this effect, a first-order differential equation was used to model the temperature; and the predicted mean vote (PMV) established in ISO 7730 allowed the calculation of the thermal comfort. In Ref. [13], a bee colony algorithm was used to minimize costs while preserving some user preferences as an acceptable range for the indoor temperature. The operation of air conditioners was planning through a particle swarm algorithm (PSO) that minimizes the energy consumption and improves the thermal comfort along a day [14]. A DSM strategy was implemented to control the thermal comfort of multiple rooms through an HVAC system [15]. In particular, the effect of adjoining rooms on temperature was considered. A MILP was first used to optimize the linear loads and then a PSO allowed the optimization of the HVAC system. Power consumption and user comfort were predicted through artificial intelligence together with surveys to the users, and a genetic algorithm was used to maximize comfort and minimize consumption in Ref. [16]. An optimal model predictive control was proposed to ensure the integrity of the art in a museum, the thermal comfort of the visitors, and the reduction in the consumption [17]. The work considered the predicted percentage of dissatisfied to evaluate comfort; and the thermal model included heat from people, adjoining rooms and convective heat transfer and thermal radiation. The authors of [18] proposed a load shifting strategy planning model (LSH-SPM) applied to an HVAC system of a house. The planning was based on a rule-based control that considered building's inside temperature and energy supplier's hourly rate scheme. To ensure thermal comfort, the ASHRAE standard was used. Also, TRNSYS (a transient system building energy modeling software) was used for thermal modeling and simulation. However, the work did not consider: i) the strategy planning as an optimization problem, ii) the electrical constraints, and iii) the thermal model (because it used a dedicated software). Finally, the review article [19] considers many papers previous to 2020 on DR that include comfort. It also presents a classification according to economic aspects, building model and comfort indices, methodology used (control, optimization), and presence of DG.

The reviewed literature show that research opportunities include applying the strategies to different buildings (especially for industry) and exploring strategies for decentralized HVAC systems. In general, most scientific publications use simplified thermal models and consider the deviation with respect to a desired temperature. In contrast, few researchers contemplate PMV, the state-space representation, and the effect of adjoining rooms. For HVAC control, most research manage the upper and lower temperatures limits of the thermostats, and some consider the use of inverters HVAC that model powers as a continuous variable.

This article proposes a demand response framework that uses a perfect prediction of outdoor temperature, heat produced by indoor sources (people, lighting, equipment, etc.), and load usage to plan the coordinated operation of air conditioning equipment throughout a day considering power and thermal constraints. It is a multi-objective optimization problem that minimizes energy cost, while ensuring an acceptable thermal comfort. The developed framework is applied to a radiotherapy and medical imaging center (MIC) placed in the province of Entre Ríos (Argentina). The application of DR strategies in air conditioning systems in healthcare facilities is a subject of growing interest, due to the great demand for energy to meet thermal comfort requirements. This topic is briefly discussed in subsection 3.1.

In contrast to the reviewed literature, the novelty of the paper relies on the management of the states (ON or OFF) of multiple units of air conditioners working in block, and on the proposed thermal model that includes effects of adjoining rooms and indoor heat sources, described through a discrete-time state-space representation. In addition, the PMV comfort formula is used in both the objective function and temperature constraints, and the optimization is carried out with a genetic algorithm. So, the main contribution of this paper is the development of a complete demand response scheme that includes: i) a multizone thermal model with discrete state-space representation, which considers the temperatures of adjoining rooms and indoor heat sources, ii) multizone thermal comfort management including a room priority scheme and power constraints, iii) evaluation of thermal cost using the ISO 7730 standard, and iv) the optimization control of multiple units of AC working in block. A genetic algorithm is developed to solve the optimization problem of the medical center case study. Two scenarios with different power demands are proposed and the strategy is compared with an on-off control for multiple AC units, with hysteresis.

The article is organized as follows: in Section II, the DSM strategies and the thermal model are presented. Section III considers the specific case study. The optimization problem and the main simulation results are presented in Section IV. Finally, the conclusions are detailed in Section V.

2. The proposed method

2.1. Demand side management

There are several DSM methods to modify the load profile [20,21], among them: Peak Clipping, Load Shifting, Strategic Growth, Valley Filling, Strategic Conservation, and Flexible Load Shape (Fig. 1). Combining peak clipping and valley filling methods results in the load shifting that requires controllable loads on the demand side. This management causes a shift from peak consumption to other time windows, but without reducing the overall energy consumption. The remaining methods are more advanced and require planning and operation to increase or decrease loads [22].

2.2. Thermal model

In the literature, there are several thermal models based on analog resistive-capacitive (RC) electric circuit. In this work, a simple RC model was used [24], with the addition of the interaction between adjoining rooms (multi-zone room interaction) and the effect of indoor heat sources (people, lighting, equipment, etc.). The analog model developed is shown in Fig. 2 (for cooling operation), where voltages correspond to temperatures and currents correspond to thermal powers. Resistances and capacities correspond to the thermal resistance and capacities, which depend on the building characteristics (size and materials) and can be determined by table or by test.

The balance of the currents in the circuit for room 1 is given by:

$$C_1\frac{dT_{i1}}{dt} = -P_{th1} + P_{s1} + \frac{(T_{out} - T_{i1})}{R_1} + \frac{(T_{i2} - T_{i1})}{R_{12}} \tag{1}$$

where T_{out} is the outdoor temperature of the building, T_{i1}, T_{i2} are the indoor temperatures of rooms 1 and 2, respectively. P_{th1} is the thermal power of the AC (for heating the direction of the source is inverted) and P_{s1} is the heat produced by indoor heat sources in room 1. Parameters (R_1, C_1), (R_2, C_2) are the thermal resistances and capacities of rooms 1 and 2, respectively, and R_{12} is the thermal resistance of the shared wall. These parameters depend on the building characteristics. Equation (1) can be rewritten as:

$$\frac{dT_{i1}}{dt} = \alpha_1 T_{i1} + \frac{T_{i2}}{R_{12}C_1} - \frac{P_{th1}}{C_1} + d_1 \tag{2}$$

where:

$$\alpha_1 = -\frac{1}{C_1}\left(\frac{1}{R_1} + \frac{1}{R_{12}}\right) \text{ and } d_1 = \frac{1}{C_1}\left(P_{s1} + \frac{T_{out}}{R_1}\right)$$

d_1 can be considered as the disturbance produced by indoor heat sources and the outdoor temperature in the system.

Similarly, the differential equation for room 2 is:

$$\frac{dT_{i2}}{dt} = \alpha_2 T_{i2} + \frac{T_{i1}}{R_{12}C_2} - \frac{P_{th2}}{C_2} + d_2 \tag{3}$$

Using the continuous state-space representation and considering that the thermal (P_{th}) and the electrical (P_{ac}) powers of an AC are related by $P_{th} = \eta P_{ac}$, where η is the coefficient of performance (CoP). The mathematical thermal model can be written as follows:

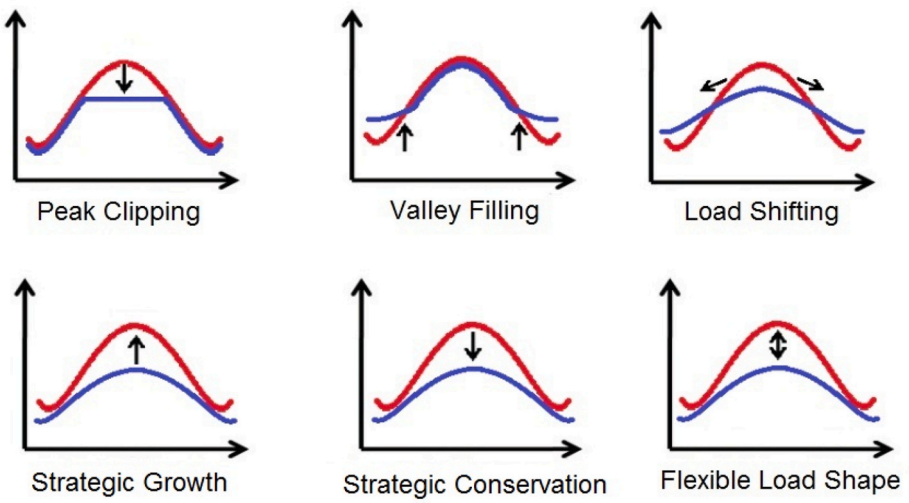

Fig. 1. Classic strategies used for DSM [23].

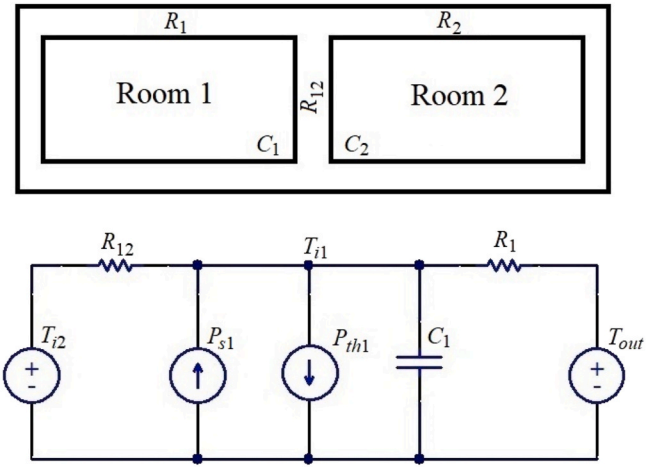

Fig. 2. Top: layout of two adjacent rooms. Bottom: RC model equivalent to a cooling system of room 1.

$$\begin{bmatrix} dT_{i1} \\ dT_{i2} \end{bmatrix} = A \begin{bmatrix} T_{i1} \\ T_{i2} \end{bmatrix} + B \begin{bmatrix} P_{ac1} \\ P_{ac2} \end{bmatrix} + D \begin{bmatrix} d_1 \\ d_2 \end{bmatrix} \tag{4}$$

where:

$$A = \begin{bmatrix} \alpha_1 & \frac{1}{R_{12}C_1} \\ \frac{1}{R_{12}C_2} & \alpha_2 \end{bmatrix}, \; B = \begin{bmatrix} -\frac{\eta}{C_1} & 0 \\ 0 & -\frac{\eta}{C_2} \end{bmatrix} \quad \text{and } D = \begin{bmatrix} 1 & 0 \\ 0 & 1 \end{bmatrix}$$

Considering a zero-order holder, Eq. (4) is discretized for a sampling time t_s.

$$T_i(k+1) = A_d T_i(k) + B_d P_{ac}(k) + D_d d(k) \tag{5}$$

$\mathbf{T_i}(k)$ is the vector of the indoor temperatures at the instant k (state variables), $\mathbf{P_{ac}}(k)$ is the vector of the air conditioner electrical power at each room (manipulated variables), and $\mathbf{d}(k)$ is the vector of the outdoor temperature and the heat produced by indoor sources (disturbances). Matrices $\mathbf{A_d}$, $\mathbf{B_d}$ and $\mathbf{D_d}$ are the discrete versions of matrices **A**, **B** and **D**.

2.3. Thermal comfort: ISO 7730

The thermal comfort proposed in ISO 7730 standard considers the use of *PMV* (Predictive Mean Vote) as a metric of thermal sensation, based on the heat balance of the human body. Thus, $PMV = 0$ implies maximum comfort, while a negative value of *PMV* indicates that the person feels cold, and a positive value indicates a warm sensation (Table 1).

The value of *PMV* is given by:

$$PMV = \left(0.303e^{-0.036M} + 0.028\right)\left\{(M-W) - 3.05\cdot 10^{-3}[5733 - 6.99(M-W) - p_a] - 0.42[(M-W) - 58.15]\right.$$
$$\left. - 1.7\cdot 10^{-5}M(5867 - p_a) - 0.0014M(34 - t_a) - 3.96\cdot 10^{-8}f_{cl}\left[(t_{cl}+273)^4 - (t_r+273)^4\right] - f_{cl}h_c(t_{cl} - t_a)\right\} \tag{6}$$

where M is the metabolism rate (W/m^2), W is the effective mechanical power (W/m^2), p_a is the water vapor partial pressure (Pa), t_a is the air temperature (°C), t_{cl} is the clothing surface temperature (°C), t_r is the mean radiant temperature (°C), f_{cl} is the clothing surface area factor and h_c is the convective heat transfer coefficient [W/(m^{2}K)]. f_{cl}, t_{cl} and h_c are solved (iteratively for t_{cl} and h_c) according to Eqs. (7)–(9), respectively [25]:

Table 1
Seven-point thermal sensation scale.

PMV	Thermal sensation
+3	Hot
+2	Warm
+1	Slightly warm
0	Neutral
−1	Slightly warm
−2	Cool
−3	Cold

$$f_{cl} = \begin{cases} 1.00 + 1.290 I_{cl} \, for \, I_{cl} \leq 0.078 \; m^2K/W \\ 1.05 + 0.645 I_{cl} \, for \, I_{cl} > 0.078 \; m^2K/W \end{cases} \tag{7}$$

$$t_{cl} = 35.7 - 0.028(M - W) - I_{cl}\left\{3.96 \cdot 10^{-8} f_{cl}\left[(t_{cl} + 273)^4 - (t_r + 273)^4\right] + f_{cl} h_c (t_{cl} - t_a)\right\} \tag{8}$$

$$h_c = \begin{cases} 2.38|t_{cl} - t_a|^{0.25} \, for \, 2.38|t_{cl} - t_a|^{0.25} > 12.1\sqrt{v_{ar}} \\ 12.1\sqrt{v_{ar}} \, for \, 2.38|t_{cl} - t_a|^{0.25} < 12.1\sqrt{v_{ar}} \end{cases} \tag{9}$$

where I_{cl} is the clothing insulation (m^2K/m), and v_{ar} is the relative air velocity (m/s).

The mean radiant temperature is considered equal to the indoor temperature [26–28]. Finally, most variables of the room can be estimated except for air temperature which can vary and is equal to the indoor temperature, $T_i = t_a$. So, *PMV* can be defined as a function of the indoor temperature.

A criterion based on the absolute deviation of the *PMV* is proposed to evaluate the thermal discomfort of a building over a given period:

$$C_{th}(T_i) = \sum_{k=1}^{n} \sum_{j=1}^{m} \mathbf{c}_j \left| \boldsymbol{PMV}_j\left(\boldsymbol{T}_{\boldsymbol{i}\, j}(k)\right)\right| \tag{10}$$

where n is the number of time intervals, m is the number of rooms and $\mathbf{PMV}_j(\mathbf{T_i}_j(k))$ is the *PMV* value of room j at instant k. The absolute deviation is used to capture the dispersion of the positive (hot) and negative (cold) *PMV* with respect to the maximum comfort value ($PMV = 0$). Through the vector $\mathbf{c}_j$ (with dimension mx1) it is possible to weigh differently the thermal cost of each room (priority thermal scheme in the objective function). The maximum comfort value is given for $C_{th} = 0$; therefore, the higher the C_{th}, the lower the comfort.

2.4. Planning objective function

The objective function is composed of the electrical energy cost and the thermal cost ($C_{th}(T_i)$). The electrical energy cost (C_{EE}) depends on the tariff scheme determined by the supplier, as well as on the total demand (vector $\mathbf{P_l}$ of n elements). The thermal cost is determined by Eq. (10) and depends on the temperature profiles of each room (matrix $\mathbf{T_i}$ of mxn). Hence, the objective function can be written as:

$$f_{obj}(P_l, T_i) = C_{EE}(P_l) + w \cdot C_{th}(T_i) \tag{11}$$

where w is a weight factor that represents a trade-off between comfort loss and money saving.

The total demand at each instant k is made up of the prediction of uncontrollable loads $\mathbf{P_{ul}}(k)$ (predicted base demand) and controllable loads (AC equipment).

$$P_l(k) = \mathbf{P_{ul}}(k) + \sum_{j=1}^{m} P_{acj}(k) \tag{12}$$

The indoor temperatures can be calculated as a function of the electrical power of the AC equipment through the thermal model of Eq. (5), using predictions of the disturbance $\mathbf{d}(k)$ (prediction of heat produced by indoor sources and forecast of outdoor temperature). So, the thermal cost depends on $\mathbf{P_{ac}}$.

$$f_{obj}(P_{ac}) = C_{EE}(P_{ac}) + w \cdot C_{th}(P_{ac}) \tag{13}$$

Eq. (13) is the objective function expressed as a function of $\mathbf{P_{ac}}$, which is the variable matrix to be optimized (mxn matrix).

2.5. Energy optimization of air conditioning

To plan the operation of the AC equipment, the heat produced by indoor sources in each room, the base demand and the outdoor temperature must be predicted. The planning aims at minimizing the electric bill while maximizing the thermal comfort, over a specified period (typically one day). The optimization problem consists of minimizing the objective function of Eq. (13) subject to both electrical constraints (demand or consumption restrictions) and thermal constraints (temperature or *PMV* restrictions).

$$minf_{obj}(P_{ac}) \tag{14}$$

s.t.

$$\sum_{j=1}^{m} P_{acj}(k) - P_{acmax}(k) \leq 0$$

$$\left|\mathbf{PMV}_j(k)\right| - \mathbf{PMV_{max}}_j \leq 0 \quad \text{for} \;\; j = 1 \;\; \text{to} \;\; m \tag{15}$$

The first restriction of Eq. (15) is an input electrical constraint and the second is a state thermal constraint. P_{acmax} is the maximum power allowed that ACs can demand, and $\mathbf{PMV_{max}}$ is the vector containing the allowed *PMV* value for each j-room (priority thermal

scheme in constraints). The absolute value of the thermal constraint is considered due to the symmetry of the *PMV* scale.

3. Case study

3.1. Thermal comfort in healthcare facilities

Although the main needs of healthcare facilities are hygiene and safety conditions, in recent years the interest in thermal comfort, energy management and efficiency have increased [29–34]. Thermal comfort is considered an important parameter of Indoor Environmental Quality (IEQ) [35]. Many works propose the evaluation of thermal comfort in health institutions using the *PMV* and the ISO 7730 standard [36,37]. The thermal comfort requirements of each room depend on the activity. The rooms with the strictest requirements are the operating rooms, considering the interval $0.5 < PMV < 0.5$ as acceptable [38].

On the other hand, higher thermal comfort requirements imply higher energy consumption. For this reason, healthcare institutions have interesting characteristics for the application of DR strategies in HVAC systems, since HVAC represent a large part of their energy consumption [39]. In addition, the operation of the medical electrical equipment responds to a patient appointment system, so load prediction is easy to perform with a certain degree of accuracy. In this sense [31,32] conduct literature reviews on energy efficiency in hospitals [40] compares different HVAC system technologies for operating rooms and [41] manages an HVAC to decrease the cost when the operating room is not being used. No articles were found that perform cost and comfort optimization of HVAC system in healthcare facilities.

In this work, the case of a radiotherapy and medical imaging center (MIC) placed in the province of Entre Ríos (Argentina) is analyzed. In this MIC, computed tomography scans, X-rays, and magnetic resonance imaging are performed, as well as radiotherapy treatments. Due to the building size ($\sim$3000 m^2), infrastructure and surroundings, the energy requirements for air conditioning are high, especially in summer. Thermal comfort is required for people and to perform certain medical studies. The MIC consists of 8 rooms (excluding offices), as shown in Fig. 3, in which rooms with the highest comfort requirements are those for treatments and diagnoses.

The analysis performed in this work is based on monthly data (average power per minute) recorded in the MIC along the year 2018.

3.2. Problem identification

According to the provincial regulations, the users whose demanded power exceeds 300 kW are individually analyzed. The provincial supplier has two tariff blocks for large demands (category T3, powers greater than 30 kW), where users are classified depending on whether their peak consumption (averaged each fifteen consecutive minutes) is less or greater than 300 kW. Users with peaks greater than 300 kW have a higher energy cost than the rest ($\approx$40%; see Table 3). Furthermore, when a demand exceeds the contracted power (with a tolerance of 5%), then the contract is automatically updated for the next four months [42]. This situation is clearly of high risk for those users who register peaks close to 300 kW. Finally, National Law N°. 27191 establishes that large users and large demands that exceed 300 kW must meet the percentage requirements of renewable energy consumed, through self-generation, or through a renewable energy purchase contract [43].

3.3. Air conditioning system and consumption

The MIC has 38 AC units (hot/cold, three-phase, 5.94 kW); 24 ACs are manageable and feed a set of ducts arranged transversely to the building line that impact on every room. The total installed power in air conditioning is $\approx$ 225 kW.

The operation of an AC changes according to the season of the year, due to the difference between the cooling/heating operations. Moreover, the largest cooling demand occurs during the afternoon, while heating is more necessary at night and in the early morning. For these reasons, the consumption profile fluctuates from month to month (Fig. 4).

Fig. 5 shows the annual variability of the demanded power. It is observed that the maxima occur in the summer months, while the average powers in summer and winter are similar. The maximum consumption detected is close to 330 kW, while demand rarely exceeds 300 kW.

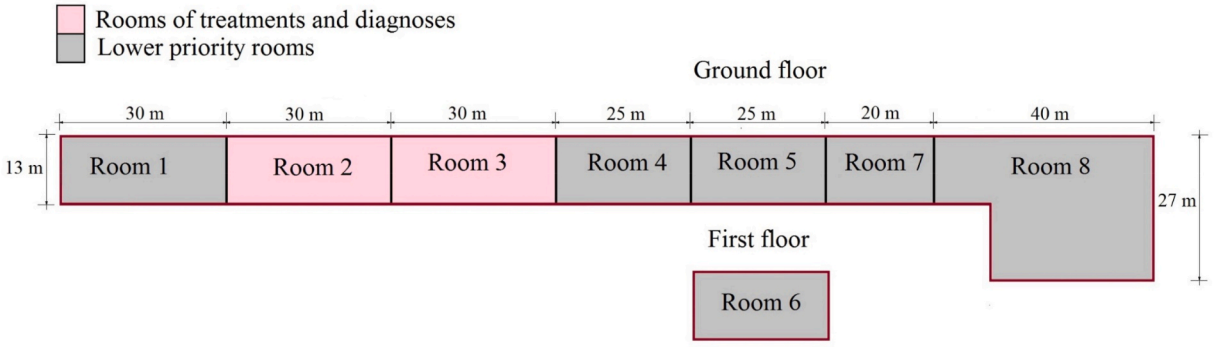

Fig. 3. Layout of the MIC.

Table 2
MIC parameters RC.

Room	WSA (m^2)	Room volume (m^3)	R (°C/kW)	C (kWh/°C)
1	219	1170	0.45	2.96
2	180	1170	0.55	2.96
3	180	1170	0.55	2.96
4	150	975	0.67	2.44
5	150	975	0.67	2.44
6	204	1170	0.46	2.96
7	120	780	0.83	2
8	291	1440	0.34	3.62

Table 3
Electricity tariff applied to the MIC [47].

Cost/Electricity rates		Time bands	Unit	Value	
				For power <300 kW	For power ≥300 kW
Fixed cost (C_F)		–	$/month	8786.41	8786.41
Power rates	Peak (R_{pp})	18h–23h	$/kW-month	677.29	677.29
	Off peak	23h–18h	$/kW-month	576.95	576.95
	Acquired	–	$/kW-month	78.32	78.32
Energy rates	Peak	18h–23h	$/kWh	2.9901	4.1576
	Valley	23h–5h	$/kWh	2.7440	3.8239
	Remaining	5h–18h	$/kWh	2.8671	3.9914

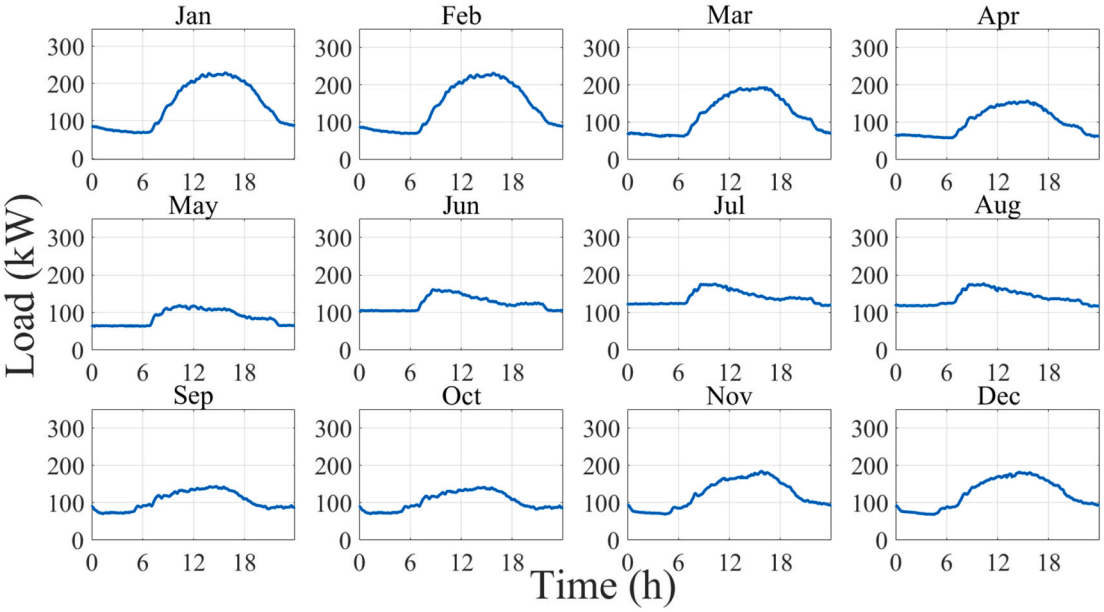

Fig. 4. MIC's average power demands in a year.

3.4. The proposed DR strategy

In this work, we propose a combination of "Load Shifting" and "Strategic Conservation" (Fig. 1), in which loads can be shifted over time and/or reduced in power according to a given scheduling strategy. The ACs can be turned on/off to keep the thermal comfort of every room within a predefined range. According to the temperature prediction and base demand, the planning strategy consists of manipulating the ACs with the aim of maintaining the comfort within the established band, while simultaneously evaluating whether the limit of 300 kW is exceeded. In such a case, the optimization procedure pursues the objective of keeping the 15 min-averaged power below the established upper-limit of 300 kW, but also considering the *PMV* constraint and the inclusion of worker/patient comfort in the objective function.

3.4.1. Thermal model of the medical center

The thermal model for the MIC is obtained by developing the equivalent RC circuits for each room (Fig. 2). For simplicity, this case

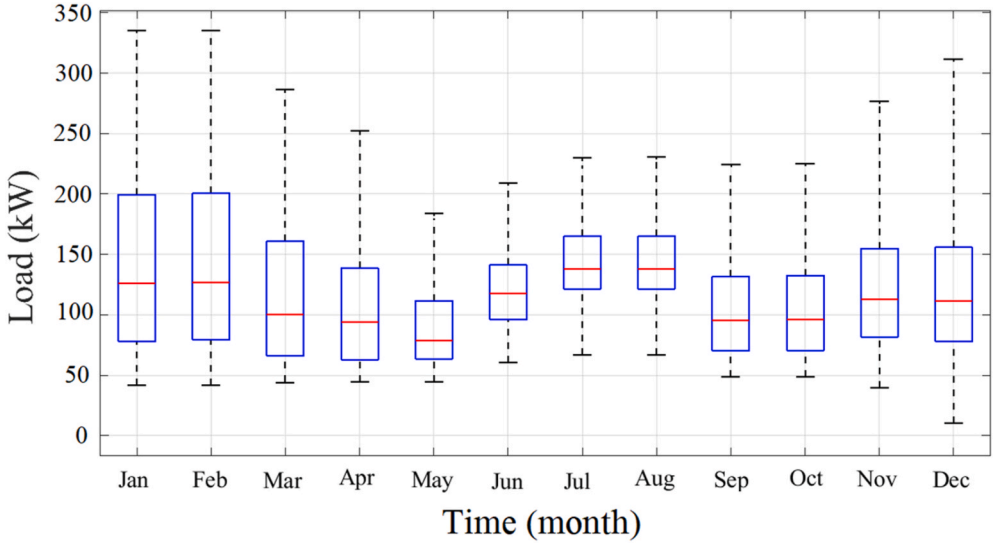

Fig. 5. Annual variability of the demanded power.

study only considers the people inside the rooms as the indoor heat source. The continuous state-space model is given by Eq. (4).

Considering $\eta = 3$ (usual CoP value in AC equipment, obtained by dividing the delivered cooling by the consumed electricity), the (diagonal) matrix **B** is:

$$B = diag\left(\frac{-3}{C_1}, \frac{-3}{C_2}, \frac{-3}{C_3}, \frac{-3}{C_4}, \frac{-3}{C_5}, \frac{-3}{C_6}, \frac{-3}{C_7}, \frac{-3}{C_8}\right)$$

Matrix **D** is the identity matrix (8 × 8 matrix), and matrix **A** is:

$$A = \begin{bmatrix} \alpha_1 & \frac{1}{C_1R_{12}} & 0 & 0 & 0 & 0 & 0 & 0 \\ \frac{1}{C_2R_{12}} & \alpha_2 & \frac{1}{C_2R_{23}} & 0 & 0 & 0 & 0 & 0 \\ 0 & \frac{1}{C_3R_{23}} & \alpha_3 & \frac{1}{C_3R_{34}} & 0 & 0 & 0 & 0 \\ 0 & 0 & \frac{1}{C_4R_{34}} & \alpha_4 & \frac{1}{C_4R_{45}} & 0 & 0 & 0 \\ 0 & 0 & 0 & \frac{1}{C_5R_{45}} & \alpha_5 & \frac{1}{C_5R_{56}} & \frac{1}{C_5R_{57}} & 0 \\ 0 & 0 & 0 & 0 & \frac{1}{C_6R_{56}} & \alpha_6 & 0 & 0 \\ 0 & 0 & 0 & 0 & \frac{1}{C_7R_{57}} & 0 & \alpha_7 & \frac{1}{C_7R_{78}} \\ 0 & 0 & 0 & 0 & 0 & 0 & \frac{1}{C_7R_{78}} & \alpha_8 \end{bmatrix}$$

For a sampling time t_s, the discrete state-space model (Eq. (5)) is obtained, where $\mathbf{T_i}(k)$, $\mathbf{P_{ac}}(k)$ and $\mathbf{d}(k)$, are (8 × 1) vectors containing the indoor temperatures, the AC electrical powers, and the disturbances (outdoor temperature and human thermal power), corresponding to each of the 8 rooms, respectively. The human thermal power is calculated on the basis of the occupancy of each room, with each person producing 120 W ($M = 60$ W/m^2 for light work, sitting) [44,45]. The R and C parameters are calculated through tables that consider the size of each room and the objects in them, the materials of the walls, floors and ceilings, the thickness of each layer that constitutes them, and the number and size of doors and windows. The methodology used to determine these parameters is described in Ref. [46]. Table 2 shows the R and C parameters, where WSA is Wall Surface Area. The thermal transmittance of the external walls is 1.022 W/m^2 °C and this was used to get the resistance of each wall.

The resistance between the walls of adjoining rooms is considered in all cases equal and its value is 8.24 °C/kW. To check the model, the resulting demand profile was compared with the actual demand profile.

3.4.2. Energy cost

For high demands (T3), the supplier establishes two hourly power bands (peak and off-peak) and three energy bands (peak, valley, and remaining). For a T3 low-voltage consumer, the costs are shown in Table 3 (current tariff of February 2022) [47].

The total monthly electricity bill (C_{EE}) is given by the sum of the fixed cost (C_F), the cost due to the demanded power (C_P) and the cost due to the consumed energy (C_E) [42], according to (16). Table 3 shows that power rates ($/kW-month) and the fixed cost ($/month) are independent of the power demanded, regardless of whether the power is less or greater than 300 kW. On the contrary, the energy rates ($/kWh) increase 40% when the power demand exceeds 300 kW, so in that case C_E represents an important percentage of C_{EE}.

$$C_{EE} = C_F + C_P + C_E \tag{16}$$

C_P is the sum of the power costs incurred during peak and off-peak hours, plus the cost of the acquired power. The acquired power (P_{ad}) is evaluated according to:

$$P_{ad} = \frac{max(P_{MRP}, P_{CP}) + max(P_{MROP}, P_{COP})}{2} \tag{17}$$

In which P_{MRP} and P_{CP} are the maximum powers registered and contracted, in peak hours; and P_{MROP} and P_{COP} the powers corresponding to off-peak.

If the demanded power is lesser than the contracted power, then the power costs during peak and off-peak hours are calculated with the contracted powers. In contrast, if the demanded power is greater than the contracted power, then a penalty is applied so that the power cost at peak hours is (C_{PP}):

$$C_{PP} = \left(P_{MRP} + \frac{P_{MRP} - P_{CP}}{2}\right) \cdot R_{PP} \tag{18}$$

where R_{PP} is the peak hour power rate. The calculation for the off-peak power cost is similar.

3.4.3. Energy optimization of the medical center

The total power demand of the MIC is composed of the AC power and the base demand (medical equipment, non-manageable ACs, lighting, computer systems, etc.). The demand for the medical equipment is estimated through a matrix that includes the powers, working hours and usage factors, according to data provided by the MIC. For this case study, the priority scheme was implemented only in the constraints, therefore the comfort cost of each room was assumed to be equal and unitary: $\mathbf{c}_j = [1,1,1,1,1,1,1,1]'$ (Eq. (10)). In addition, $w = 1700$ (Eq. (11)) was selected after several simulations. Then, the optimization problem is formulated as follows:

$$minf_{obj}(P_{ac}) \tag{19}$$

s.t.

$$Co_1(k) = \sum_{j=1}^{m} P_{acj}(k) - P_{av}(k) \leq 0$$

$$Co_2(k) = \left|PMV_j(k)\right| - PMV_{max_j} \leq 0 \quad \text{for } j = 1 \text{ to } 8 \tag{20}$$

Equation (20) represents the optimization problem constraints. Co_1 establishes the maximum power that the AC can demand. P_{av} is the power available for air conditioning at instant k, which is obtained by subtracting the base demand predicted power from the established power limit (300 kW). Co_2 represent the thermal restriction with the two-level priority scheme of Fig. 3, where $\mathbf{PMV_{max}} = [1,0.75,0.75,1,1,1,1,1]'$. This scheme makes it possible to maintain comfort in the higher priority rooms ($-0.75 \leq PMV \leq 0.75$) at the expense of comfort in the lower priority rooms ($-1 \leq PMV \leq 1$), on days with high outdoor temperatures and base demand. Co_2 defines the maximum PMV range in the rooms which implies the maximum tolerated discomfort. PMV values are calculated as in subsection 2.3 with $M = 60$ W/m^2 (considering seated and quiet people), $W = 0$ W/m^2, $I_{cl} = 0.2$ m^{2}K/W (for summer clothes) and $v_{ar} = 0.1$ m/s p_a is calculated from computing the saturation pressure of water and assuming the relative humidity equal to 50% [12,45]. The same parameterization is used for low and high priority rooms, so that PMV values are controlled only by indoor temperatures. Otherwise, thermal comfort could be controlled by considering some parameters as variables, according to Eqs. (6)–(9). For example, PMV can be decreased by reducing activity (lower values of M), wearing light clothing (lower values of I_{cl}), increasing effective mechanical power (higher values of W), or, in this case, increasing the relative air velocity (higher values of v_{ar}). Increasing relative air velocity can increase or decrease the PMV value, depending on the values of other parameters.

As the supplier establishes daily tariff blocks, the strategy is a daily minimization of the monthly minimization of the billing cost, therefore the number of intervals is $n = \frac{24}{t_s}$ (t_s in hours).

3.5. Evaluation of the case study strategy

The proposed strategy is compared against a non-optimized strategy, based on two different daily cases. The non-optimized strategy maintains the indoor room temperature in the range [20 °C - 25 °C], regardless of energy consumption and using an improved and coordinated on-off control for several AC units with hysteresis. Case 1 considers a daily demand profile where the total

power is always lesser than 300 kW for both strategies, while Case 2 considers that the demand is greater than 300 kW for non-optimized strategies. Both cases use the same base demand, the same outdoor temperature profile (typical for a hot summer day, when the MIC usually has the highest power demand), and the same occupancy of people/patients per room.

Fig. 5 shows that power peaks exceeding 300 kW occur rarely during the year. For this reason, to calculate the economic cost (monthly) it is assumed that the demand and daily temperature described in the previous cases are repeated over 5 days in January. The remaining days respond to a real mean MIC profile, taken from Fig. 4.

4. Simulation tests

4.1. Simulation parameters

The simulation was performed in MATLAB through a proprietary code. A sampling time $t_s = 15$ min (equal to the measurement time used by the supplier) was considered, thus $n = 96$ intervals.

The number of optimization variables is determined by the number of rooms, the times that ACs can be switched on/off in an hour (four times since $t_s = 15$ min), and the working hours of the MIC (typically, 18 h a day, from 6:00 a.m. to 12:00 p.m.). Thus, the number of variables is $8 \times 4 \times 18 = 576$. Additionally, every room has three ACs of 5.94 kW each. Then, depending on the number of simultaneously operative ACs, the power per room can take four values: {0, 5.94, 11.88, 17.82} kW, which respectively correspond to {0%, 33%, 66%, 100%} of the nominal capacity per room. Under these conditions, the number of combinations is 4^{576}, which implies a huge search space.

The optimization is done using a genetic algorithm (GA) that includes *PMV* constraints and available power. The GA toolbox of MATLAB was used, and the parameters of the GA were obtained by simulation: number of iterations: 4000, initial population: 300, crossover: 0.8 and number of best individuals: 25.

4.2. Simulation results and discussion

In simulations without optimization, the coordinated on-off control generates a vector indicating how many ACs should be turned on/off for each room, along the day. Since both cases without optimization have the same control and output temperature, then they have similar temperature profiles. In simulations with optimization, this vector is adopted as a member of the initial GA population.

Figs. 6–12 show optimized and non-optimized power demand and indoor temperature and *PMV* for each case. Fig. 6 shows the power profiles of both cases, with and without optimization. In Case 1, the power profiles of both strategies are lower than the constraint (300 kW). There is no reduction in power demand of the optimized strategy versus the non-optimized strategy due to the high weighting of thermal cost in the objective function ($w = 1700$). In the non-optimized Case 2, the power exceeds 300 kW because the power base demand is 43 kW higher than in Case 1. Consequently, the GA (optimized strategy) considers the electrical power constraint and generates a better demand profile. Fig. 7 shows the temperature profiles obtained in Case 1. The optimized AC strategy improves internal temperature profiles over the non-optimized one maintaining room temperatures close to 22.6 °C (equivalent to $PMV = 0$), without increasing power demand. Fig. 8 shows the thermal comfort of rooms with low priority and Fig. 9 shows the thermal comfort of rooms with high priority during a day. In all rooms, the comfort constraints are met for the case with optimization.

Fig. 10 shows the temperature profiles of Case 2 indicating that the temperature range of the rooms increases under the optimization strategy, particularly at peak demand times, but does not exceed the imposed constraints. The different thermal dynamics of each room observed in Figs. 7 and 10 are due to the different dimensions and construction characteristics of the rooms. Figs. 11 and 12 show the thermal comfort and its constraint. Every room also fulfills the comfort requirement in this case.

For the optimized strategy of Case 2, the analysis of Figs. 6 and 10 shows a smoother consume keeping the power slightly below 300 kW, and a small increase in energy consumption in the periods preceding the peak that allows cutting power peaks by turning off the air conditioners. Furthermore, the temperature increases during the peak and is close to the upper constraint.

The results of the comparison of both cases with the non-optimized strategy are summarized in Table 4. Under the conditions mentioned above, in Case 1 there are slight differences in energy consumption and electrical cost between both strategies, but there is a substantial improvement in the total thermal comfort (reduction of 40.6% for optimized strategy). In Case 2, the application of the optimization strategy would produce a monthly savings of $142681, which is equivalent to a bill reduction of 16.8%. This saving occurred because in the situation with optimization the power demand never exceeds 300 kW while in the situation without optimization, the demand exceeds 300 kW, and the energy tariff becomes more expensive increasing the billing costs. The overall energy consumption for both strategies, in Case 2, is similar, but the reduction of the total thermal cost when applying the optimized strategy is 29.2%.

In economic terms, the benefits obtained from the implementation of the strategy depend on the outdoor temperature and the base demand profile. If the total demand exceeds 300 kW at least once in the month the tariff applied to the MIC is the maximum due to the power peak, and the supplier automatically set this tariff for the next three months. The ACs management allows peak shaving when demand exceeds 300 kW.

The optimized strategy in Case 2 reduced the electrical cost through peak shaving, limiting the power demand to less than 300 kW, so the tariff applied by the energy supplier is the cheapest (Table 3). The energy consumed with this strategy is not necessarily less than the non-optimized, as it is shown in Fig. 6. In the non-optimized scenario, when the demand exceeds 300 kW, the tariff of energy is 40% higher and this produces the savings of 16.8% (Table 4). This important saving was obtained while thermal comfort was improved, and energy consumption was maintained. Note that the optimization objectives are to improve thermal comfort and reduce electrical cost, while energy consumption will not necessarily be reduced. In this sense, the optimization performs a trade-off between the two conflicting objectives, weighted by w.

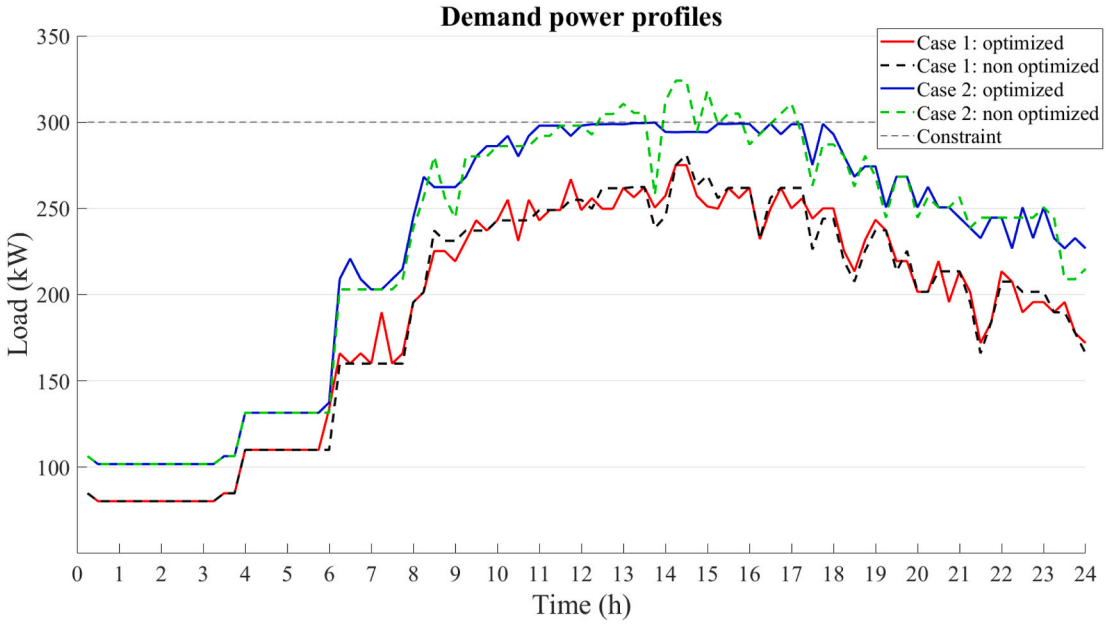

Fig. 6. Optimized and non-optimized power demand for each case.

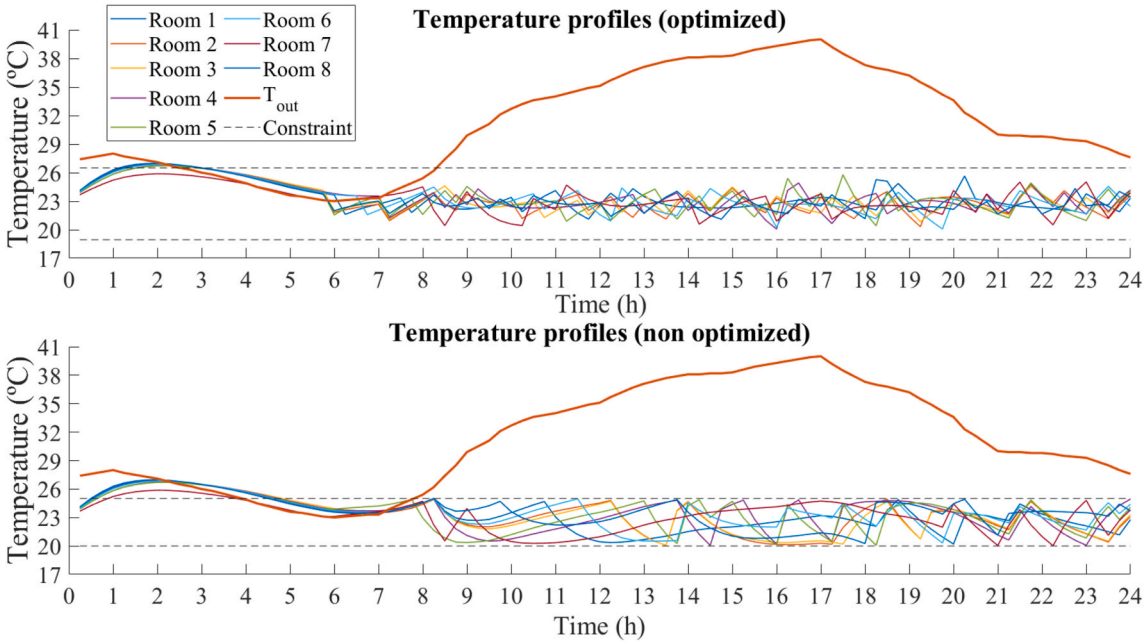

Fig. 7. Case 1: profiles of daily indoor temperatures.

In both cases, the optimizations achieve a win-win strategy, due to the reduction of the electrical cost and the improvement of thermal comfort with respect to the improved and coordinated AC on-off control.

5. Conclusions

In this paper, a low computational and economic cost solution was proposed for planning and managing air conditioning systems. The application of this DR approach in HVAC systems is a useful methodology to reduce billing costs and improve comfort, since it only requires a computer center and remote-control devices for the equipment to be managed. Furthermore, HVAC systems are ideal for the implementation of DR strategies due to their high-power demand and high consumption, and for the possibility to their operation

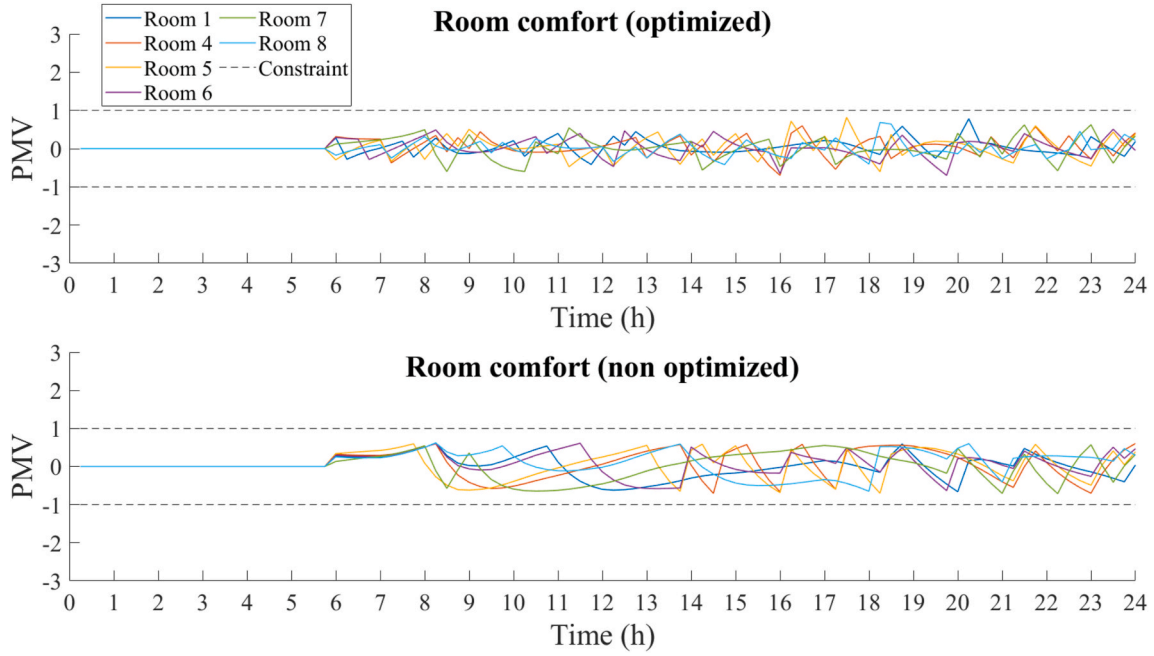

Fig. 8. Case 1: daily evolution of the PMV of rooms 1, 4, 5, 6, 7 and 8 (low priority rooms).

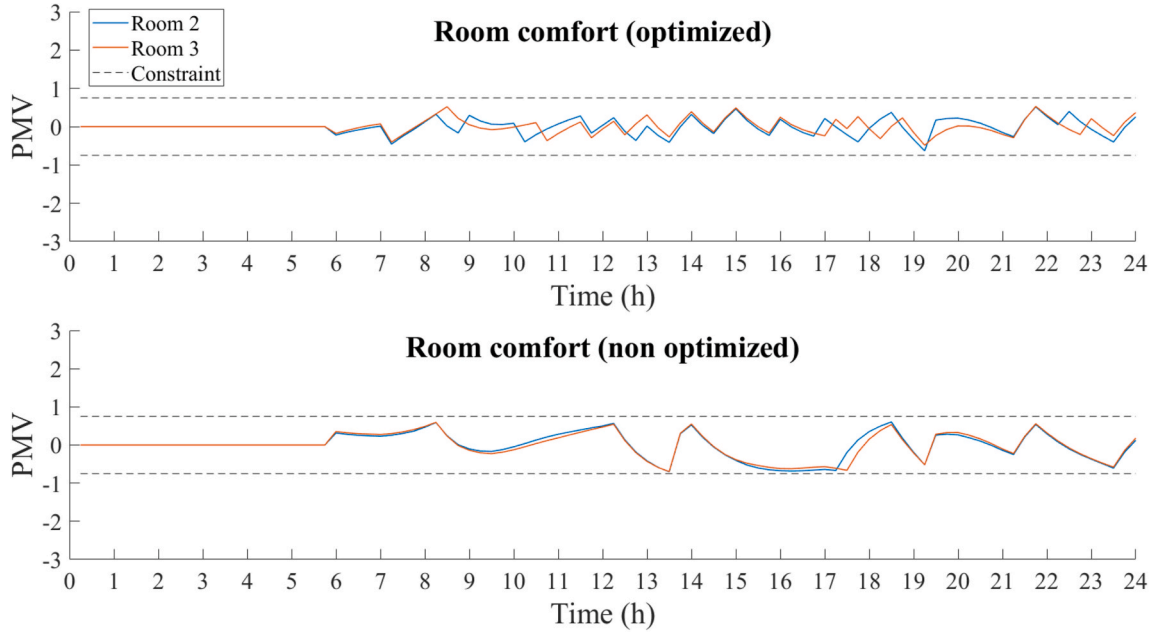

Fig. 9. Case 1: daily evolution of the PMV of rooms 2 and 3 (high priority rooms).

control based on a thermal model and the prediction of weather variables.

The developed framework can be used in different applications: i) single or multizone air conditioning planning, ii) single or multi-unit operation working in block, iii) optimization problems of different natures (constrained and unconstrained, continuous, or discrete) solved with metaheuristic algorithms, iv) different optimization objectives such as minimizing billing cost, energy consumption, power demand or thermal discomfort (defining the constraints and the objective function of the problem properly), and v) multi-level room priority schemes.

The framework was applied to the case study of a radiotherapy and medical imaging center located in Argentina. The savings that the strategy can provide to the MIC depends on the base demand and the outdoor temperature due to the formulation of the

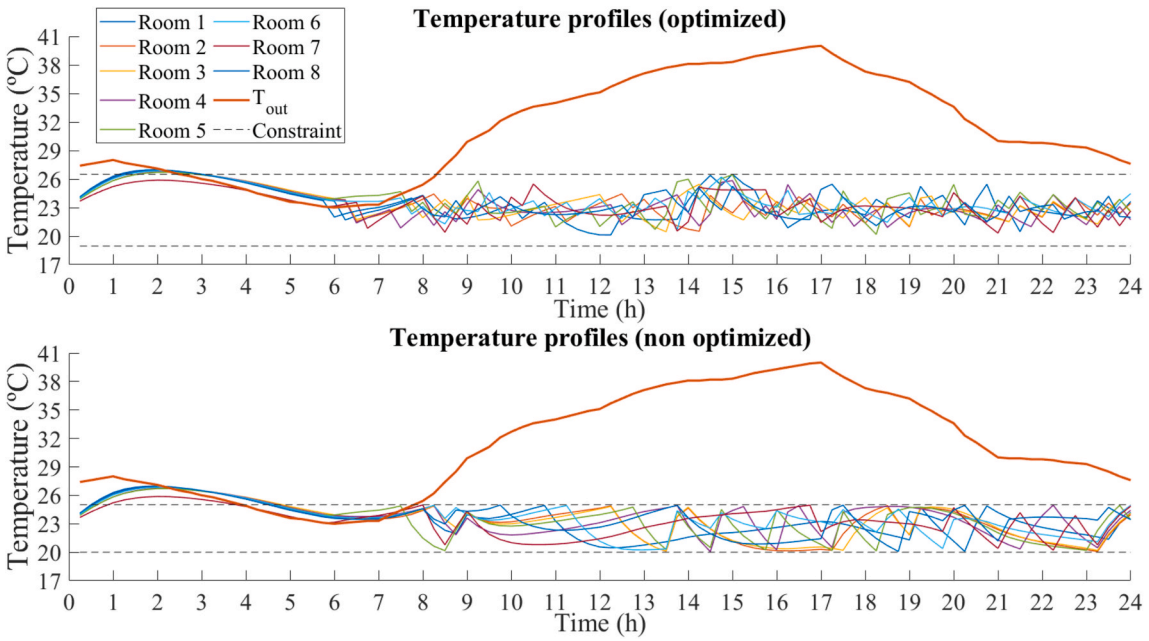

Fig. 10. Case 2: profiles of daily indoor temperatures.

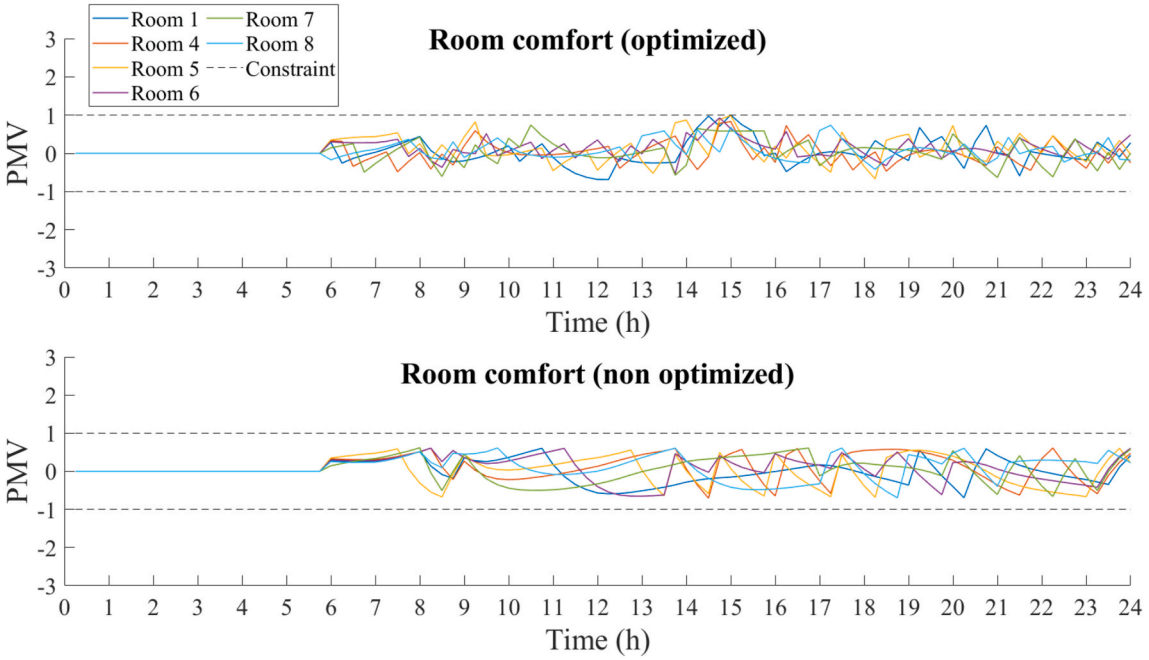

Fig. 11. Case 2: daily evolution of the PMV of rooms 1, 4, 5, 6, 7 and 8 (low priority rooms).

optimization problem. In this sense, the simulations show that the optimized strategy produces, in the two cases analyzed (Case 1 with a low base demand, and Case 2 with a high base demand, both cases with high temperature), a noticeable improvement in thermal comfort. For Case 1, the improvement in comfort was 40.6%, without increasing the electrical cost (due to the value of w used, that balances thermal comfort with cost savings). For Case 2, the comfort improvement was 29.2% and the electrical cost decreased 16.8%. This saving is due to the power constraint of 300 kW, so that the application of the expensive tariff of the energy supplier is avoided. In addition, the energy consumption for each case was the same for both the optimized and non-optimized strategies. This is because the goal of the optimization was to achieve economic savings, not to minimize energy consumption.

Finally, the case study and the framework have a strong regional impact and demonstrate that is an interesting solution for large

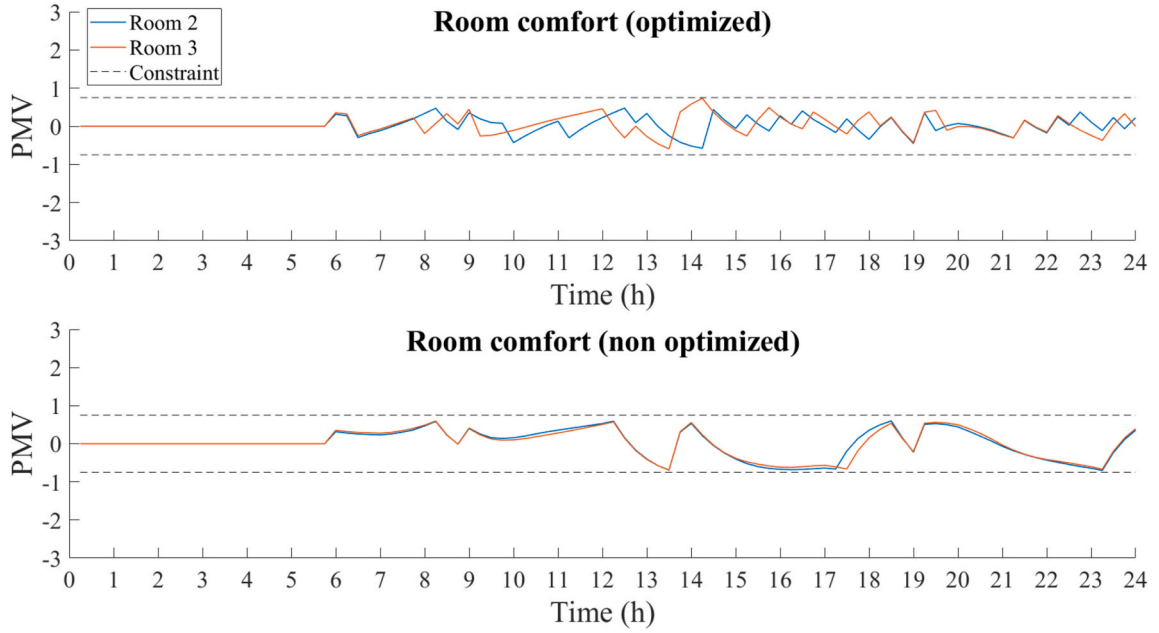

Fig. 12. Case 2: daily evolution of the PMV of rooms 2 and 3 (high priority rooms).

Table 4
Economic results of the two planning strategies for Cases 1 and 2.

Case		Peak power (kW)	Energy (kWh)	Cost	
				Electrical C_{EE} ($)	Thermal C_{th}
1	Optimized	275.0	104973	669542	110.7
	Non optimized	281.0	104928	669990	186.3
2	Optimized	299.7	109474	704911	136.3
	Non optimized	324.0	109451	847592	192.7

energy users with demands over 300 kW. The approach can easily be extended to other cases with multizone thermal models, *PMV* constraint and power constraint. Future research may consider disturbance prediction, real-time control application, other indoor heat sources (besides people), and radiant temperature asymmetry.

Author statement

Sergio Bragagnolo: Conceptualization, Formal analysis, Investigation, Methodology, Software, Validation Writing- Original draft preparation. **Rodrigo Schierloh**: Conceptualization, Formal analysis, Investigation, Methodology, Software, Validation Writing- Original draft preparation. **Jorge Vega**: Methodology, Supervision, Writing- Reviewing and Editing. **Jorge C. Vaschetti**: Methodology, Supervision, Writing- Reviewing and Editing.

Declaration of competing interest

The authors declare that they have no known competing financial interests or personal relationships that could have appeared to influence the work reported in this paper.

Data availability

The authors do not have permission to share data.

Acknowledgments

J.R.V. acknowledges the financial support by CONICET (PIP 251–2015), UTN (PID 5151-2019), CIESE (UTN), and CYTED 717RT0533 - MEIHAPER (Hybrid Intelligent Electric Microgrids with High Penetration of Renewable Energies).

References

[1] S. Belhaiza, U. Baroudi, A game theoretic model for smart grids demand management, IEEE Trans. Smart Grid 6 (3) (May 2015) 1386–1393, https://doi.org/10.1109/TSG.2014.2376632.

[2] M. Hussain, Y. Gao, A review of demand response in an efficient smart grid environment, Electr. J. 31 (5) (Jun. 2018) 55–63, https://doi.org/10.1016/j.tej.2018.06.003.

[3] M. Kong, B. Dong, R. Zhang, Z. O'Neill, HVAC energy savings, thermal comfort and air quality for occupant-centric control through a side-by-side experimental study, Appl. Energy 306 (Jan. 2022), 117987, https://doi.org/10.1016/j.apenergy.2021.117987.

[4] IEA, The Future of Cooling, 2018. https://www.iea.org/reports/the-future-of-cooling. (Accessed 25 June 2021).

[5] M.A. Fayazbakhsh, F. Bagheri, M. Bahrami, A resistance–capacitance model for real-time calculation of cooling load in HVAC-R systems, J. Therm. Sci. Eng. Appl. 7 (4) (2015), 041008, https://doi.org/10.1115/1.4030640.

[6] G. Huang, J. Yang, C. Wei, Cost-Effective and Comfort-Aware Electricity Scheduling for Home Energy Management System, 2016, pp. 453–460, https://doi.org/10.1109/BDCloud-SocialCom-SustainCom.2016.73.

[7] Z. Liang, D. Bian, X. Zhang, D. Shi, R. Diao, Z. Wang, Optimal energy management for commercial buildings considering comprehensive comfort levels in a retail electricity market, Appl. Energy 236 (2019) 916–926.

[8] W. Fan, N. Liu, J. Zhang, Multi-objective optimization model for energy management of household micro-grids participating in demand response, in: 2015 IEEE Innovative Smart Grid Technologies-Asia (ISGT ASIA), 2015, pp. 1–6, https://doi.org/10.1109/ISGT-Asia.2015.7387040.

[9] N. Li, L. Chen, S.H. Low, Optimal Demand Response Based on Utility Maximization in Power Networks, 2011, pp. 1–8, https://doi.org/10.1109/PES.2011.6039082.

[10] A. Ajao, J. Luo, Z. Liang, Q.H. Alsafasfeh, W. Su, Intelligent Home Energy Management System for Distributed Renewable Generators, Dispatchable Residential Loads and Distributed Energy Storage Devices, 2017, pp. 1–6, https://doi.org/10.1109/IREC.2017.7926040.

[11] F. Wang, et al., Multi-objective optimization model of source–load–storage synergetic dispatch for a building energy management system based on tou price demand response, IEEE Trans. Ind. Appl. 54 (2) (2017) 1017–1028, https://doi.org/10.1109/TIA.2017.2781639.

[12] D.L. Ha, S. Ploix, E. Zamai, M. Jacomino, A home automation system to improve household energy control, IFAC Proc. Vol. 39 (3) (2006) 15–20, https://doi.org/10.3182/20060517-3-FR-2903.00011.

[13] Y. Zhang, P. Zeng, C. Zang, Optimization Algorithm for Home Energy Management System Based on Artificial Bee Colony in Smart Grid, 2015, pp. 734–740, https://doi.org/10.1109/CYBER.2015.7288033.

[14] R. Kuroha, Y. Fujimoto, W. Hirohashi, Y. Amano, S. Tanabe, Y. Hayashi, Operation planning method for home air-conditioners considering characteristics of installation environment, Energy Build. 177 (Oct. 2018) 351–362, https://doi.org/10.1016/j.enbuild.2018.08.015.

[15] Y. Gao, S. Li, X. Fu, W. Dong, B. Lu, Z. Li, Energy management and demand response with intelligent learning for multi-thermal-zone buildings, Energy 210 (2020), 118411.

[16] K. Amasyali, N.M. El-Gohary, Real data-driven occupant-behavior optimization for reduced energy consumption and improved comfort, Appl. Energy 302 (2021), 117276.

[17] E. Schito, P. Conti, L. Urbanucci, D. Testi, Multi-objective optimization of HVAC control in museum environment for artwork preservation, visitors' thermal comfort and energy efficiency, Build. Environ. 180 (2020), 107018.

[18] N. Alibabaei, A.S. Fung, K. Raahemifar, A. Moghimi, Effects of intelligent strategy planning models on residential HVAC system energy demand and cost during the heating and cooling seasons, Appl. Energy 185 (2017) 29–43.

[19] A.L. da Fonseca, K.M. Chvatal, R.A. Fernandes, Thermal comfort maintenance in demand response programs: a critical review, Renew. Sustain. Energy Rev. 141 (2021), 110847.

[20] T. Logenthiran, D. Srinivasan, T.Z. Shun, Demand side management in smart grid using heuristic optimization, IEEE Trans. Smart Grid 3 (3) (2012) 1244–1252, https://doi.org/10.1109/TSG.2012.2195686.

[21] Y. Liu, C. Yuen, S. Huang, N.U. Hassan, X. Wang, S. Xie, Peak-to-average ratio constrained demand-side management with consumer's preference in residential smart grid, IEEE J. Sel. Top. Signal Process. 8 (6) (Dec. 2014) 1084–1097, https://doi.org/10.1109/JSTSP.2014.2332301.

[22] B. Lokeshgupta, A. Sadhukhan, S. Sivasubramani, Multi-objective optimization for demand side management in a smart grid environment, in: 2017 7th International Conference on Power Systems (ICPS), Dec. 2017, pp. 200–205, https://doi.org/10.1109/ICPES.2017.8387293.

[23] A.R. Vidal, L.A. Jacobs, L.S. Batista, An evolutionary approach for the demand side management optimization in smart grid, in: IEEE Symposium on Computational Intelligence Applications in Smart Grid (CIASG), 2014, pp. 1–7, https://doi.org/10.1109/CIASG.2014.7011561.

[24] F. Amara, K. Agbossou, A. Cardenas, Y. Dubé, S. Kelouwani, Comparison and simulation of building thermal models for effective energy management, Smart Grid Renew. Energy (Jan. 2015) 95–112, https://doi.org/10.4236/sgre.2015.64009, 06.

[25] International Standard Organization, ISO 7730 (2005): Ergonomics of the Thermal Environment – Analytical Determination and Interpretation of Thermal Comfort Using Calculation of the PMV and PPD Indices and Local Thermal Comfort Criteria, 2005.

[26] M. Langner, K. Scherber, W.R. Endlicher, Indoor Heat Stress: an Assessment of Human Bioclimate Using the UTCI in Different Buildings in Berlin, 144th ed., DE: Gesellschaft für Erdkunde zu Berlin, 2014 https://doi.org/10.12854/erde-144-18.

[27] O. Kaynakli, M. Kilic, Investigation of indoor thermal comfort under transient conditions, Build. Environ. 40 (2) (Feb. 2005) 165–174, https://doi.org/10.1016/j.buildenv.2004.05.010.

[28] S. Godbole, Investigating the Relationship between Mean Radiant Temperature (MRT) and Predicted Mean Vote (PMV): A Case Study in a University Building, 2018. Retrieved from, http://urn.kb.se/resolve?urn=urn:nbn:se:kth:diva-235927.

[29] P.F. da C. Pereira, E.E. Broday, A.A. de P. Xavier, Thermal comfort applied in hospital environments: a literature review, Appl. Sci. 10 (20) (Oct. 2020) 7030, https://doi.org/10.3390/app10207030.

[30] J. Khodakarami, N. Nasrollahi, Thermal comfort in hospitals – a literature review, Renew. Sustain. Energy Rev. 16 (6) (Aug. 2012) 4071–4077, https://doi.org/10.1016/j.rser.2012.03.054.

[31] A. Gatea, M.F.M. Batcha, J. Taweekun, Energy efficiency and thermal comfort in hospital buildings: a review, Int. J. Integrated. Eng. 12 (3) (2020) 33–41.

[32] A. Teke, O. Timur, Assessing the energy efficiency improvement potentials of HVAC systems considering economic and environmental aspects at the hospitals, Renew. Sustain. Energy Rev. 33 (2014) 224–235.

[33] M. Khan, M.J. Thaheem, M. Khan, A. Maqsoom, M. Zeeshan, Thermal comfort and ventilation conditions in healthcare facilities-part 1: an assessment of Indoor Environmental Quality (IEQ), Environ. Eng. Manag. J. 19 (6) (2020).

[34] M. Khan, M.J. Thaheem, M. Khan, A. Maqsoom, M. Zeeshan, Thermal comfort and ventilation conditions in healthcare facilities-part 2: improving Indoor Environment Quality (ieq) through ventilation retrofitting, Environ. Eng. Manag. J. 19 (11) (2020).

[35] International Standard Organization, ISO 17772-1 (2017). Energy Performance of Buildings — Indoor Environmental Quality — Part 1: Indoor Environmental Input Parameters for the Design and Assessment of Energy Performance of Buildings, 2017.

[36] A. Pourshaghaghy, M. Omidvari, Examination of thermal comfort in a hospital using PMV–PPD model, Appl. Ergon. 43 (6) (Nov. 2012) 1089–1095, https://doi.org/10.1016/j.apergo.2012.03.010.

[37] B.S. Alotaibi, R. Codinhoto, D. Albadra, S. Lo, Combined multi-attribute inpatient thermal comfort requirements in hospitals: a designer's assessment method, J. Build. Eng. 42 (Oct. 2021), 103039, https://doi.org/10.1016/j.jobe.2021.103039.

[38] C. Liu, G. Zhou, H. Li, Analysis of thermal environment in a hospital operating room, Procedia Eng. 121 (2015) 735–742, https://doi.org/10.1016/j.proeng.2015.09.021.

[39] P.A. Hohne, K. Kusakana, B.P. Numbi, Improving energy efficiency of thermal processes in healthcare institutions: a review on the latest sustainable energy management strategies, Energies 13 (3) (Jan. 2020) 569, https://doi.org/10.3390/en13030569.

[40] T.-Y. Chien, C.-C. Liang, F.-J. Wu, C.-T. Chen, T.-H. Pan, G.-H. Wan, Comparative analysis of energy consumption, indoor thermal–hygrometric conditions, and air quality for HVAC, LDAC, and RDAC systems used in operating rooms, Appl. Sci. 10 (11) (2020) 3721.
[41] A. Cacabelos-Reyes, J.L. López-González, A. González-Gil, L. Febrero-Garrido, P. Eguía-Oller, E. Granada-Álvarez, Assessing the energy demand reduction in a surgical suite by optimizing the HVAC operation during off-use periods, Appl. Sci. 10 (7) (2020) 2233.
[42] EPRE, Resolución N° 168/16 Anexo I: Régimen Tarifario, 2016. Available: http://epre.gov.ar/web/wp-content/uploads/2016/11/Resolucion-168-16_A-_I.pdf.
[43] J.L. Godoy, R.M. Schierloh, J. Vega, Economic Evaluation of Micro-grids with Renewable Generation, 2018, pp. 1–6.
[44] R. Riemer, A. Shapiro, Biomechanical energy harvesting from human motion: theory, state of the art, design guidelines, and future directions, J. NeuroEng. Rehabil. 8 (1) (2011) 22, https://doi.org/10.1186/1743-0003-8-22.
[45] R.T. Oğulata, The effect of thermal insulation of clothing on human thermal comfort, Fibres Text. East. Eur. 15 (2) (2007). Art. no. 2.
[46] Norma IRAM 11601, Acondicionamiento térmico de edificios, Métodos de cálculo, 1996.
[47] ENERSA, Situación Tarifaria, 2022. https://www.enersa.com.ar/informacion-comercial/. (Accessed 28 January 2022).